Materials Physics and Mechanics 47 (2021) 40-51 Received: November 10, 2020

ON BUCKLING INDUCED BY A CHEMICAL REACTION

V.O. Shtegman[1,2*], A.V. Morozov[3], A.B. Freidin[1,2,4], W.H. Müller[3]

[1]Institute for Problems in Mechanical Engineering of the Russian Academy of Sciences, St. Petersburg, Russia

[2]Saint Petersburg University, St. Petersburg, Russia

[3]Technische Universität Berlin, Berlin, Germany

[4]Peter the Great St. Petersburg Polytechnic University, St. Petersburg, Russia

*e-mail: vshtegman@gmail.com

Abstract. This study is concerned with the modeling of plate buckling induced by a chemical reaction and is inspired by the observation that buckling may be a mechanism of stress relaxation in Si-based anodes in Li-ion batteries. A chemical reaction is localized at a sharp interface and accompanied by transformation strains, which produce internal stresses. If external supports restrict the deformation of the plate, buckling may occur. At the same time, mechanical stresses affect the kinetics of the reaction. The chemical affinity tensor concept allows us to couple the stresses with the chemical reaction rate. We formulate a coupled problem for a plate with two reaction fronts and find the critical thickness of the transformed material and the time before buckling. The influence of the material and geometrical parameters on the buckling occurrence and the time until buckling is studied

Keywords: mechanochemistry, plate buckling, chemical affinity tensor, chemical reaction kinetics, diffusion, internal stresses

1. Introduction

The increase of temperature, strains induced by phase and chemical transformations, swelling, etc., may result in a significant volumetric expansion of structural elements. If external supports or loadings restrict the deformation of the structural elements, buckling may occur. Buckling of a rod made of a shape memory alloy (see, e.g. [1,2] and reference therein) represents an example of the loss of stability induced by a phase transformation strain. In [3] and [4] it is reported on buckling and a numerical simulation of surface delamination and wrinkling of bi-layered composite thin films. Buckling-induced fracture and delamination of the supercapacitor due to the charge transfer was studied in [5]. In [6] the authors considered buckling of a hydrogel plate on a stiff substrate depending on the swelling ratio.

In the present paper, we are interested in the buckling induced by chemical transformations. An important example is the lithiation of silicon in Li-ion batteries. The reaction between Li and crystalline Si is a two-phase process [7,8], which may occur at a sharp interface [9,10]. Lithiated Si phase is produced according to the chemical reaction:

$$\mathrm{Si} + x\mathrm{Li} \rightarrow \mathrm{Li}_x\mathrm{Si}, \tag{1}$$

where the maximal theoretical value of x is 4.4 ($Li_{22}Si_5$). However, highly lithiated amorphous silicon practically forms the metastable phase $Li_{15}Si_4$ with $x = 3.75$, see [11] and references therein. The reaction is accompanied by volume expansion up to 300% [12], which, in turn, produces internal stresses that may lead to the loss of the stability and buckling of the elements of battery anodes. In [13] the authors studied lithiation-induced buckling of wire-based electrodes; in [14] a cylindrical Si anode is considered, and the critical length is

http://dx.doi.org/10.18149/MPM.4712021_4

determined; in [15] the effect of radial and axial diffusion on the buckling of nanowires is investigated, and the critical length is determined.

In the examples mentioned above buckling looks like a negative phenomenon, which means the loss of the load-bearing capacity of a structural element. However, the stresses may retard and even block chemical reactions, in particular, the lithiation reaction [7,16]. In this case, buckling may be a useful mechanism of stress relaxation in structural elements of Si-based anodes. Baggetto *et al*. [17] performed an experimental study in which the authors fabricated a honeycomb periodic structure of the Si anode, which is schematically shown in Fig. 1 (a), and studied its storage capacity and cycle stability.

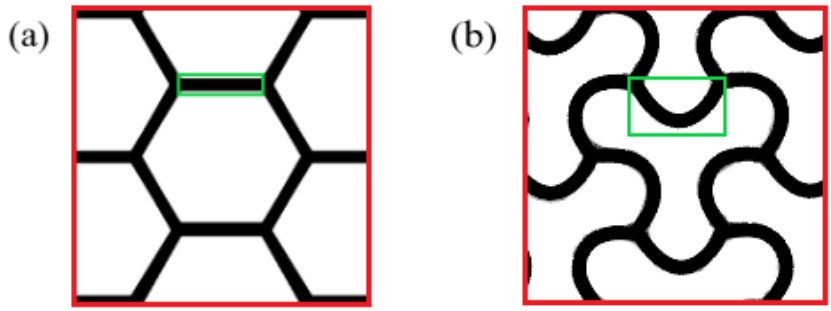

Fig. 1. Schematic representation of the Si-based honeycomb structured anode: (a) unlithiated; (b) lithiated. Design from [17]

Due to the volumetric expansion induced by a chemical reaction at full lithiation the Si honeycombs adopt their morphology, see Fig. 1 (b), such that the stored elastic energy is released via buckling of the periodic structure. Later this process was studied numerically in [18,19] where the authors modeled a lithiation-induced deformation of various periodic structures. In these studies, the lithiation process was modeled as a non-stationary diffusion flow of Li ions into the Si matrix and transformation strains were incrementally applied as a function of Li concentration. Therefore, in this model, lithiation of the Si anode influence the internal stresses but not vice versa. However, as already mentioned, the lithiation reaction can be retarded or even blocked by internal stresses produced by the chemical transformation [7,16]. Moreover, the reaction can be controlled by the reaction rate rather than by the diffusivity of the reactant see, *e.g.*, [20,21] and references therein.

Our current study is inspired by the honeycomb-structured design for Si-based anode for which we want to take into account such a chemo-mechanical coupling. The honeycomb vertices do not move during lithiation and only rotate after buckling [17] (Fig. 1). Therefore, we consider the buckling of a simply supported plate as a model problem. We make a first step toward modeling the lithiation-induced buckling process in terms of a stress-dependent chemical reaction by using the chemical affinity tensor concept [22]. This concept allows to couple directly mechanical stresses and the reaction rate in a thermodynamically sound manner. Strictly speaking, Si is a viscoelastic material [23-25]. However, in this work, we are concerned with a qualitative study of structural element buckling induced by a chemical reaction. Thus, we start from the small strain approximation and linear elastic material models.

The paper is organized as follows. In Section 2, we give an overview of the chemical reaction fronts kinetics based on a chemical affinity tensor concept. To demonstrate a scenario of the stability consideration based on an analytical solution of the mechanochemistry problem we simplify the problem and consider a small strain approach and linear elastic constituents. Then, in Section 3, the model problem of a plate undergoing a chemical reaction is considered and the kinetics of the reaction fronts is described. The critical thickness of the transformed material layer and the time before buckling are found in Section 4. The influence

of various model parameters on time until buckling is studied. Hence, we demonstrate that the problem statement includes formulation a reaction front kinetics, finding the critical front position at which the stability loss may occur, and finding the time prior to the stability loss. Conclusions and an outlook are presented in Section 5. It is noted that the critical thickness and time before buckling may represent the initial condition for the post-buckling analysis.

2. Modeling kinetics of the chemical reaction

We consider a chemical reaction of the following type:

$$n_- B_- + n_* B_* \to n_+ B_+, \tag{2}$$

where n_-, n_*, and n_+ are the stoichiometric coefficients, B_-, B_*, and B_+ are the chemical formulae of the constituents of the reaction, and the subscripts "$-$", "$*$", and "$+$" refer to the initial solid material, diffusing reactant, and solid reaction product, respectively. During further analysis the stoichiometric coefficients n_*, n_-, n_+ are normalized by n_* ($n_- \longrightarrow n_-/n_*$, $n_+ \longrightarrow n_+/n_*$). It is assumed that the chemical reaction is localized at the reaction front and the diffusing reactant is fully consumed by the reaction.

The chemical reaction is accompanied by a volume expansion. An elementary volume of initial material $\mathrm{d}V_- = n_- M_-/\rho_-$ transforms into an elementary volume of transformed material $\mathrm{d}V_+ = n_+ M_+/\rho_+$, where $M_\pm$ and $\rho_\pm$ are the molar masses and reference mass densities of the constituents $B_\pm$, respectively. The diffusing constituent can produce additional volume $\xi M_*/\rho_*$ inside of the material B_+, where M_* and ρ_* are the molar mass and reference mass density of the diffusing reactant, respectively. The parameter ξ characterizes the deformational interaction between the reactants B_* and B_+ and depends on the diffusion mechanism and saturability of the diffusing reactant B_* in the reaction product B_+. Then the ratio of volumes of materials on both sides of the reaction front, if they were stress-free (the transformation strain), is given by the formula [26]:

$$J_{\mathrm{ch}} = \frac{n_+ M_+/\rho_+ + \xi M_*/\rho_*}{n_- M_-/\rho_-}. \tag{3}$$

The case $\xi = 0$ corresponds to the solid skeleton approach (diffusion is not accompanied by the change of volume) and the case $\xi = 1$ corresponds to adding the volumes of the reaction product and the diffusing reactant. Generally speaking, J_{ch} may depend on the concentration of the diffusing constituent, if $\xi \neq 0$, but for the sake of brevity we further consider this strain as a material parameter.

The transformation strain results in mechanical stresses which in turn affect the reaction rate. To find stresses and strains one has to solve the equilibrium equation

$$\nabla \cdot \boldsymbol{\sigma} = \mathbf{0} \tag{4}$$

with boundary and interface conditions

$$\mathbf{u}|_{\Omega_1} = \mathbf{u}_0, \qquad \boldsymbol{\sigma}|_{\Omega_2} = \mathbf{t}_0\,, \tag{5}$$

$$[\![\mathbf{u}]\!]|_\Gamma = 0, \qquad [\![\boldsymbol{\sigma}]\!]|_\Gamma \cdot \mathbf{n} = \mathbf{0}, \tag{6}$$

where $\mathbf{u}_0$ and $\mathbf{t}_0$ are the displacement and traction prescribed at the parts Ω_1 and Ω_2 of the outer boundary of the body, Γ is the reaction front. We consider linear elastic solid constituents with constitutive relations

$$\boldsymbol{\sigma}_- = \mathbf{C}_- : \boldsymbol{\varepsilon}_-, \qquad \boldsymbol{\sigma}_+ = \mathbf{C}_+ : (\boldsymbol{\varepsilon}_+ - \boldsymbol{\varepsilon}_{\mathrm{ch}}), \tag{7}$$

where $\mathbf{C}_\pm$ are the stiffness tensors and $\boldsymbol{\varepsilon}^{\mathrm{ch}}$ is the chemical transformation strain:

$$\mathbf{C}_\pm = \lambda_\pm \mathbf{E}\mathbf{E} + 2\mu_\pm \mathbf{I} \;\; \boldsymbol{\varepsilon}_{\mathrm{ch}} = \varepsilon_{\mathrm{ch}} \mathbf{E} = \left(J_{\mathrm{ch}}^{1/3} - 1\right)\mathbf{E}, \tag{8}$$

where $\lambda_\pm$ and $\mu_\pm$ are the Lamé parameters, and $\mathbf{E}$ and $\mathbf{I}$ are the second and fourth order unit tensors, respectively.

The chemical reaction (2) requires the supply of the diffusing reactant through the reaction product to the reaction front. We neglect the initial stage of the diffusion of B_* prior to the start of the reaction and separation of the reaction front from the outer boundary of the

body. We also assume that the diffusion process is much faster than the velocity of the reaction front propagation. Then the stationary diffusion can be described by the equation

$$\Delta c = 0 \tag{9}$$

with boundary conditions

$$\begin{aligned} &D\mathbf{n}\cdot\nabla c - a_*(c_* - c) = 0 \text{ at } \Omega_+, \\ &D\mathbf{n}\cdot\nabla c + \omega_n = 0 \text{ at } \Gamma, \end{aligned} \tag{10}$$

where a_* is the surface mass transfer coefficient, c_* is the solubility of B_* in B_+, Ω_+ is the outer boundary of the domain occupied by the transformed material, and ω_n is the reaction rate at a surface element with the normal $\mathbf{n}$ directed outward the domain occupied by the reaction product.

The first boundary condition in (10) states that if the solubility c_* is reached then the supply of the diffusing reactant stops. The second boundary condition results from the mass balance at the reaction front and states that all the diffusing reactant is consumed by the reaction.

In this work, the chemical affinity tensor concept is used for modeling the reaction front kinetics. The chemical affinity tensor was derived as the direct consequence of the mass balance, linear momentum balance, energy balance, and the second law of thermodynamics in the form of the Clausius-Duhem inequality written for moving reaction front [20], see also [27,28]. The validity of the chemical affinity tensor approach for the modeling of the reaction front kinetics was demonstrated in bodies of various rheology [26-31].

The kinetic equation used by Glansdorff and Prigogine [32] can be reformulated for the reaction rate ω_n at the area element with the normal $\mathbf{n}$ as follows [22]:

$$\omega_n = k_* c \left\{1 - \exp\left(-\frac{A_{nn}}{RT}\right)\right\}, \tag{11}$$

where k_* is a kinetic coefficient, c is the partial molar concentration of the diffusing reactant, R is the universal gas constant, T is the current temperature, and A_{nn} is the normal component of the chemical affinity tensor. The normal component of the reaction front velocity, W_n, can be obtained from the mass balance at the reaction front:

$$W_n = \frac{n_- M_-}{\rho_-}\omega_n. \tag{12}$$

Effects of stresses and strains on the reaction front kinetics are accounted for via their influence on the chemical affinity tensor. It can be shown [28] that the expression for the normal component of the chemical affinity tensor within a small stain approximation takes the following form:

$$A_{nn} = \frac{n_- M_-}{\rho_-}\chi + RT\ln\left(\frac{c}{c_*}\right). \tag{13}$$

Here c_* is the reference concentration of the diffusing constituent taken as solubility, χ is defined by the contributions of mechanical and chemical energies:

$$\chi = \gamma + \frac{1}{2}\boldsymbol{\sigma}_-:\boldsymbol{\varepsilon}_- - \frac{1}{2}\boldsymbol{\sigma}_+:(\boldsymbol{\varepsilon}_+ - \boldsymbol{\varepsilon}_{\mathrm{ch}}) + \boldsymbol{\sigma}_-:(\boldsymbol{\varepsilon}_+ - \boldsymbol{\varepsilon}_-), \tag{14}$$

where γ is the energy parameter defined by the chemical energies of the stress-free solid constituents and the reference energy of the diffusing constituent. It depends on temperature, and it is taken as a material parameter in the present consideration. Then, the reaction rate (11) can be expressed as

$$\omega_n = k_*(c - c_*\varkappa), \tag{15}$$

where $\varkappa$ represents the influence of mechanical stresses and is defined as

$$\varkappa = \exp\left(-\frac{n_- M_-}{\rho_-}\frac{\chi}{RT}\right). \tag{16}$$

Hence, one has a coupling between mechanics, diffusion, and chemical reaction. In addition, effects of mechanical stresses can be accounted for through the stress-dependent

diffusivity and the cross effects of stress gradient in the diffusion flux, see, *e.g.*, [33-36]. However, in the present work, we focus only on the influence of stresses on the reaction rate and consequences of the reaction front propagation for the loss of stability of a structural element.

3. Buckling of a plate due to a chemical reaction

We consider a plate of the length a, width b, and thickness $2H$ undergoing a chemical reaction. The plate is simply supported at the edges $x = \pm a/2$. The upper and lower sides $y = \pm H$ are traction-free. The diffusing reactant is supplied through the upper and lower sides, and the chemical reaction starts simultaneously from both sides and propagates towards the middle plane (Fig. 2). Further, we assume a plane strain formulation with $b \gg a$ and $\varepsilon_z^{\pm} = 0$. It is also assumed that the reaction front is planar before buckling, the top and bottom layers of the transformed material have the same thickness h and the plate is symmetric with respect to the middle plane.

The Hooke laws (7) take the following form in terms of Young's moduli $E_{\pm}$ and Poisson's ratios $\nu_{\pm}$:

$$\varepsilon_y^+ - \varepsilon_{\text{ch}} = \frac{1}{E_+}\left(\sigma_y^+ - \nu_+(\sigma_z^+ + \sigma_x^+)\right),$$
$$\varepsilon_y^- = \frac{1}{E_-}\left(\sigma_y^- - \nu_-(\sigma_z^- + \sigma_x^-)\right). \tag{17}$$

The expressions for $\varepsilon_x^{\pm}$ and $\varepsilon_z^{\pm}$ follow from (17) by cyclic permutations of x, y, and z. Due to the pinned boundary conditions we have $\varepsilon_x^{\pm} = 0$. Since the upper and lower sides of the plate are traction free and the traction continuity condition $[\![\sigma_y]\!]\big|_{\text{y=±(H−h)}} = 0$ holds at the reaction fronts, $\sigma_y^{\pm} = 0$. Then from (17) it follows that non-zero components of the stress tensor are:

$$\sigma_x^+ = \sigma_z^+ = \varepsilon_{\text{ch}} \frac{E_+}{1 - \nu_+}. \tag{18}$$

These stresses are the internal stresses produced by the transformation strain. The stresses do not depend on the front position in the considered case. Then χ does not depend on the thickness of the new material layer,

$$\chi = \gamma - \varepsilon_{\text{ch}}^2 \frac{E_+}{1 - \nu_+}. \tag{19}$$

The chemical reaction can proceed only if $\omega_n > 0$, which holds only if $\chi > 0$, *i.e.*, $\gamma/\gamma_* > 1$, where $\gamma_* = \varepsilon_{\text{ch}}^2 E_+/(1 - \nu_+)$ defines the critical value of the energy parameter γ. The latter inequality represents the competition between the inputs of the chemical energies and the mechanical energy produced by the transformation strain. It should be noted that in the considered case γ_* does not depend on the reaction front position.

Due to the symmetry of the problem with respect to the middle plane $y = 0$ it is enough to consider only one reaction front and one diffusion problem before the buckling occurs. Further, consider the reaction front $y = H - h$. The diffusion equation (9) becomes

$$\frac{\mathrm{d}^2 c}{\mathrm{d}y^2} = 0, \qquad y \in [H - h, H]. \tag{20}$$

The solution is $c(y) = C_1 y + C_2$, where the constants C_1 and C_2 can be found from the boundary conditions

$$D\frac{\mathrm{d}c}{\mathrm{d}y} - a_*(c_* - c) = 0 \text{ at } y = H, \tag{21}$$

$$-D\frac{\mathrm{d}c}{\mathrm{d}y}+\omega_n=0 \text{ at } y=H-h,$$

where ω_n is determined by (15) with χ given by (19). The concentration of the diffusing reactant at the reaction front is

$$c(y)|_{y=H-h}=\frac{1+\varkappa k_*\left(\frac{1}{\alpha_*}+\frac{h}{D}\right)}{1+k_*\left(\frac{1}{\alpha_*}+\frac{h}{D}\right)}c_*. \tag{22}$$

Once the mechanical and diffusion problems are solved and the reaction rate is found, one can obtain the normal component of the reaction front velocity W_n as a function of the interface position using (12):

$$W_n(h)=\frac{dh}{dt}=\frac{n_-M_-}{\rho_-}\frac{c_*(1-\varkappa)}{\frac{1}{k_*}+\left(\frac{1}{\alpha_*}+\frac{H}{D}\zeta\right)}, \tag{23}$$

where $\zeta=h/H$ is the relative thickness of the transformed layer. This gives the dependence of the reaction front position on time, *i.e.*, the kinetics of the front. Integrating (23) one derives the time of reaching the relative thickness ζ:

$$t(\zeta)=H\int_0^{\zeta}\frac{1}{W_n(\zeta)}\mathrm{d}\zeta=\frac{\rho_-}{n_-M_-}\frac{\left(\frac{1}{k_*}+\frac{1}{\alpha_*}\right)\zeta+\frac{H}{2D}\zeta^2}{c_*(1-\varkappa)}H. \tag{24}$$

The time is inversely proportional to the kinetic coefficient k_*, the mass transfer coefficient α_*, and the diffusivity D. Internal stresses produced by the transformation strain affect the reaction front kinetics via the parameter $\varkappa$ which increases if χ increases. Then from (16), (19) and (24), it is seen how the time of reaching ζ increases if the ratio γ/γ_* decreases.

4. Critical force and time before buckling

As mentioned earlier, we consider a plate with simply supported edges $x=\pm a/2$ (Fig. 2). During propagation of the chemical reaction front the reaction force at the supports increases and the bending stiffness of the plate changes. The reaction force can be calculated as

$$R_x(h)=\int_{-H}^{-h}\sigma_{x+}\mathrm{d}y+\int_{-h}^{h}\sigma_{x-}\mathrm{d}y+\int_{h}^{H}\sigma_{x+}\mathrm{d}y. \tag{25}$$

Substitution of the stresses (18) gives

$$R_x(h)=2\varepsilon_{\mathrm{ch}}\frac{E_+}{1-\nu_+}h. \tag{26}$$

The critical buckling load for the considered plate is

$$N_{cr}(h)=D_{eff}(h)\frac{\pi^2}{a^2}, \tag{27}$$

where the effective bending stiffness D_{eff} of a plate is given by

$$D_{\mathrm{eff}}(h)=\int_{-H}^{H}y^2\,C\,\mathrm{d}y=\frac{2}{3}C_+(H^3-(H-h)^3)+\frac{2}{3}C_-(H-h)^3 \tag{28}$$

with $C_\pm=E_\pm/(1-\nu_\pm^2)$, see, *e.g.*, [37].

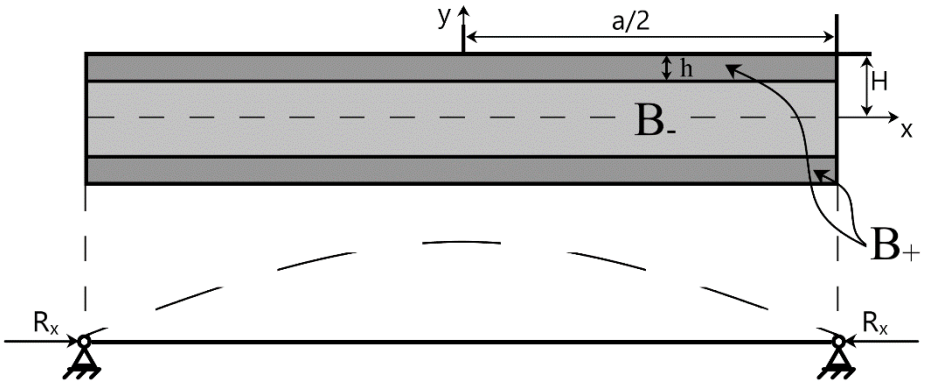

Fig. 2. Schematic representation of a plate

The buckling criterion is the equality of the reaction force and the critical buckling load, *i.e.*, $R_x(h_{cr}) = N_{cr}(h_{cr})$, where h_{cr} is the thickness of the transformed layer at which buckling occurs, further referred to as the critical thickness. Substitution of (26)-(28) into the buckling criterion leads to the equation

$$\left(\frac{C_-}{C_+} - 1\right)\eta_{\mathrm{cr}}^3 + G\eta_{\mathrm{cr}} + (1 - G) = 0, \tag{29}$$

where $\eta_{\mathrm{cr}} = 1 - \zeta_{cr}$, $\zeta_{\mathrm{cr}} = h_{\mathrm{cr}}/H$, the dimensionless parameter G depends on the chemical transformation strain, Poisson's ratio and the geometrical dimensions of the plate in the considered case:

$$G = 3\varepsilon_{\mathrm{ch}}(1 + \nu_+)\frac{a^2}{\pi^2 H^2}. \tag{30}$$

Buckling occurs if the solution of (29) is in range $\eta_{\mathrm{cr}} \in [0, 1]$. It can be shown that such a root exists and that it is unique if $G \geq 1$.

For further calculations, we use geometrical dimensions taken from [17] and material parameters from [30] are compiled in Table 1.

Table 1. Parameters used in the calculations

Parameter	a [m]	H [m]	E_- [GPa]	E_+ [GPa]	ν_-	ν_+
Value	$11.6\cdot10^{-6}$	$0.125\cdot10^{-6}$	134	41	0.22	0.26
Parameter	γ [J/m^3]	D [m^2/s]	c_* [mol/m^3]	k_* [m/s]	α_* [m/s]	$\varepsilon_{\mathrm{ch}}$
Value	$5\cdot10^{9}$	10^{-12}	$5.3\cdot10^{-2}$	$8.6\cdot10^{-8}$	$2\cdot10^{-6}$	0.05

Dependencies of the relative reaction force (26) and relative critical force (27) on the relative thickness of the transformed material are shown in Fig. 3. At the initial stage of the reaction, the thickness of the transformed layer is less than the critical value h_{cr} and the inequality $R_x(h) < N_{\mathrm{cr}}(h)$ holds. While the chemical reaction front propagates, the reaction force at the supports increases, and the bending stiffness of the plate decreases. Thus, buckling occurs at $h = h_{\mathrm{cr}}$.

The dependencies of the critical relative thickness ζ_{cr} on the parameter G for various values of the ratio C_-/C_+ are shown in Fig. 4. The zoomed-in part confirmed that the solution of the equation (29) exists if $G \geq 1$. The ratio C_-/C_+ represents the influence of the material parameters on the bending stiffness of a plate. It is defined by the elastic moduli of both solid constituents, but at fixed G it can be changed by varying E_-. Therefore, various curves in Fig. 4 can be treated as the dependencies $\zeta_{\mathrm{cr}}(G)$ constructed for various values of Young's modulus of the initial material.

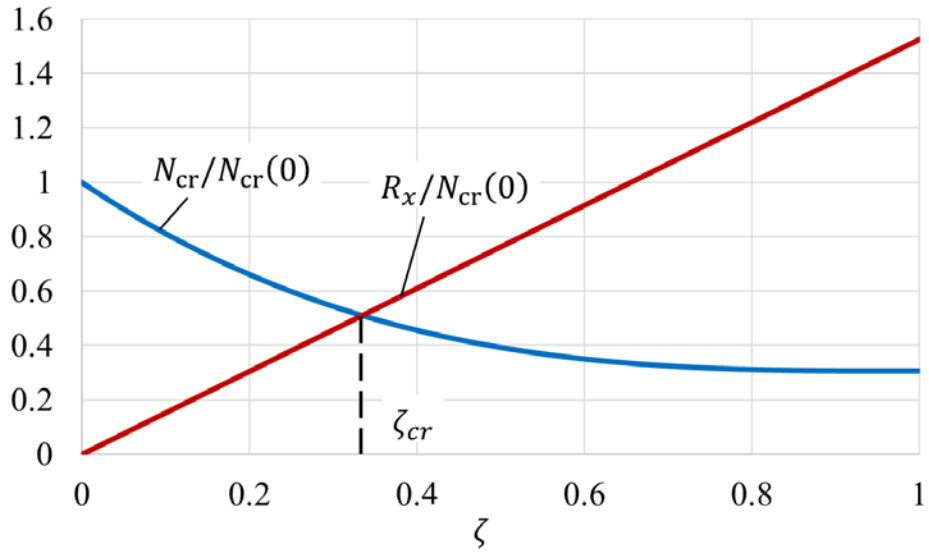

Fig. 3. Critical load and reaction force at the supports as a function of the relative thickness of transformed material layer

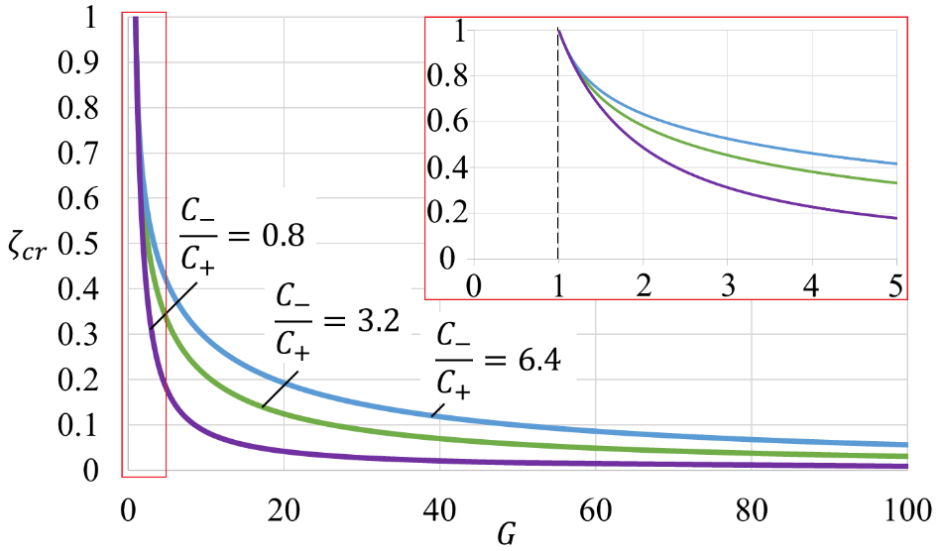

Fig. 4. Dependencies of the critical thickness ζ_{cr} of the transformed material layer on parameter G at various relations of elastic moduli of the solid constituents

For given transformation strain and elastic moduli, by adjusting the ratio a^2/H^2, one can achieve the buckling at desirable ζ_{cr}. If the critical thickness is found, one can calculate the time t_{cr} until buckling from (24). The dependencies of the time until buckling on the parameter G at various values of the energy parameter γ are shown in Fig. 5. The calculations were performed for the parameters from Table 1 for which $C_-/C_+ = 3.2$, $a^2/H^2 = 538$.

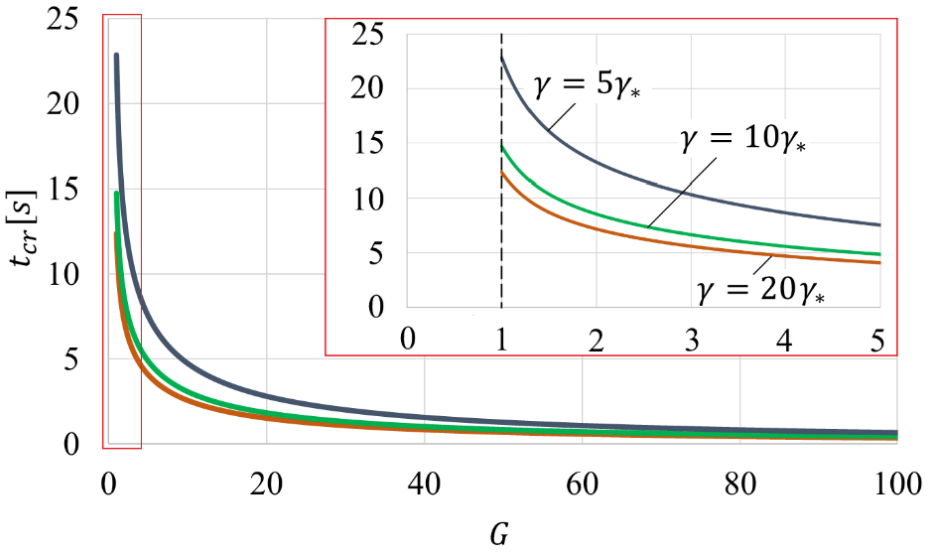

Fig. 5. Dependencies of the time prior buckling on the parameter G at various γ

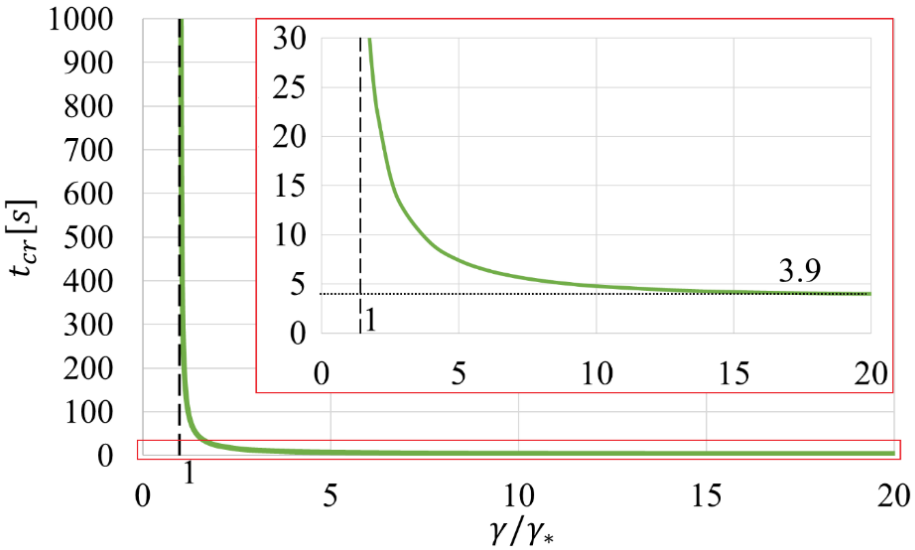

Fig. 6. Dependence of the time until buckling on the chemical energy parameter

The dependence of the time until buckling on the energy parameter is shown in Fig. 6. If the energy parameter γ defined by the chemical energies is comparable to the contribution of the mechanical energy, then the influence of the internal stresses on time until buckling becomes noticeable. In order to decrease the time until buckling one can increase the energy parameter by changing the temperature. However, the temperature may produce thermal stresses affecting the kinetics of the reaction. Also, note that in the present study linear-elastic materials were considered, and buckling was the only mechanism of stress relaxation. In the case of viscoelastic or viscoplastic behaviors, stress may relax due to inelastic deformations. Buckling may not occur due to this relaxation, but the front propagation might be temporary blocked by the remaining stresses. This may lead to uneven front propagation with retardation/acceleration and blocking stages (see, *e.g.*, [30,38]).

5. Conclusion

In this paper, the buckling of the plate due to a chemical reaction was studied in dependence on the reaction front position. For the first time, the reaction front kinetics was modeled based on the chemical affinity tensor in application to the buckling problem. Expressions of the

reaction force at the supports and critical load were obtained in dependence on the thickness of the transformed material layer. Then the critical thickness of the transformed layer and the time before buckling were determined. It was studied how the transformation strain, elastic moduli, the ratio of the plate thickness to the length affect the critical thickness of the transformed material and time until buckling. It was also examined how the energy parameter and reaction kinetic parameters affect the critical time.

Therefore, with the described procedure, one can estimate whether buckling occurs and, if it does, calculate the critical thickness of the transformed material layer and the time before buckling. Once the plate buckles, the stresses, and strains make the problem no longer symmetric. The further kinetics of the reaction fronts during the post-buckling requires special investigations for which the critical thickness and critical time represent the initial condition for the post-buckling analysis.

Acknowledgements*. The authors appreciate the financial support from the joint project of the Russian Foundation for Basic Research (RFBR, 17-51-12055) and Deutsche Forschungsgemeinschaft (DFG, MU 1752/47-1).*

References

[1] Movchan AA, Kazarina SA, Sil'chenko AL. Buckling of a rod with a circular cross section induced by a direct thermoelastic martensitic transformation. *Russian Metallurgy (Metally).* 2020;2020(4): 298-304.

[2] Dumanskii SA, Movchan AA. Loss of stability of a rod from a shape-memory alloy caused by reverse martensitic transformation. *Mechanics of Solids.* 2019;54(6): 929-940.

[3] Nikravesh S, Ryu D, Shen Y. Instabilities of Thin Films on a Compliant Substrate: Direct Numerical Simulations from Surface Wrinkling to Global Buckling, *Sci. Rep.* 2020;10(1): 1-19.

[4] Mei H, Huang R, Chung J, Stafford C, Yu H-H. Buckling modes of elastic thin films on elastic substrates. *Applied Physics Letters.* 2007;90(15): 151902.

[5] Yang F. Analysis of charging-induced structural damage in electrochemical systems. *Physical Chemistry Chemical Physics.* 2017;19(10): 7072-7077.

[6] Ilseng A, Prot V, Skallerud BH, Stokke BT. Buckling initiation in layered hydrogels during transient swelling. *Journal of the Mechanics and Physics of Solids.* 2019;128: 219-238.

[7] McDowell MT, Lee SW, Harris JT, Korgel BA, Wang C, Nix WD, Cui Y. In situ TEM of two-phase lithiation of amorphous silicon nanospheres. *Nano Letters.* 2013;13(2): 758-764.

[8] Liu XH, Fan F, Yang H, Zhang S, Huang JY, Zhu T. Self-Limiting Lithiation in Silicon Nanowires. *ACSNANO.* 2013;7(2): 1495-1503.

[9] Liu XH, Wang JW, Huang S, Fan F, Huang X, Liu Y, Krylyuk S, Yoo J, Dayeh SA, Davydov AV, Mao SX. In-situ atomic-scale imaging of electrochemical lithiation in silicon, *Nature Nanotech.* 2012;7: 749-756.

[10] Liu XH, Zhong L, Huang S, Mao SX, Zhu T, Huang JY. Size-Dependent Fracture of Silicon Nanoparticles During Lithiation. *ACSNANO.* 2012;6(2): 1522-1531.

[11] McDowell MT, Lee SW, Nix WD, Cui Y. 25th Anniversary Article: Understanding the Lithiation of Silicon and Other Alloying Anodes for Lithium-Ion Batteries. *Advanced Materials.* 2013;25(36): 4966-4985.

[12] Kasavajjula U, Wang C, Appleby AJ. Nano- and bulk-silicon-based insertion anodes for lithium-ion secondary cells. *Journal of Power Sources.* 2007;163(2): 1003-1039.

[13] Zhang, K, Li Y, Wu J, Zheng B, Yang F. Lithiation-induced buckling of wire-based electrodes in lithium-ion batteries: A phase-field model coupled with large deformation. *International Journal of Solids and Structures.* 2018;144-145: 289-300.

[14] Chakraborty J, Please CP, Goriely A, Chapman SJ. Combining mechanical and chemical effects in the deformation and failure of a cylindrical electrode particle in a Li-ion battery. *International Journal of Solids and Structures.* 2015;54: 66-81.

[15] Zhang K, Li Y, Zheng B, Wu G, Wu J, Yang F. Large deformation analysis of diffusion-induced buckling of nanowires in lithium-ion batteries. *International Journal of Solids and Structures.* 2017;108: 230-243.

[16] van Havenbergh K, Turner S, Marx N, van Tendeloo G. The mechanical behavior during (de)lithiation of coated silicon nanoparticles as anode material for lithium-ion batteries studied by in-situ transmission electron microscopy. *Energy Technology.* 2016;4(8): 1005-1012.

[17] Baggetto L, Danilov D, Notten PHL. Honeycomb-structured silicon: Remarkable morphological changes induced by electrochemical (De)lithiation. *Advanced Materials.* 2011;23(13): 1563-1566.

[18] Laptev AM, Malede YC, Duan S, Mücke R, Danilov D, Notten PHL, Guillon O. Modeling large patterned deflection during lithiation of micro-structured silicon. *Extreme Mechanics Letters.* 2017;15: 145-150.

[19] Duan S, Laptev AM, Mücke R, Danilov DL, Notten PHL, Guillon O. Topological optimization of patterned silicon anode by finite element analysis. *Mechanics Research Communications.* 2019;97: 63-69.

[20] Zhao K, Pharr M, Wan Q, Wang W, Kaxiras E, Vlassak J, Suo Z. Concurrent reaction and plasticity during initial lithiation of crystalline silicon in lithium-ion batteries. *J Electrochem Soc*. 2012;159: A238-A243.

[21] Jia Z, Li T. Stress-modulated driving force for lithiation reaction in hollow nano-anodes. *J. Power Sources*. 2015;275: 866-876.

[22] Freidin A. Chemical affinity tensor and stress-assist chemical reactions front propagation in solids. In: *Proceedings of the ASME 2013 International Mechanical Engineering Congress and Exposition*. American Society of Mechanical Engineers; 2013. p.V009T10A102.

[23] Berla LA, Lee SW, Cui Y, Nix WD. Mechanical behavior of electrochemically lithiated silicon. *Journal of Power Sources*. 2015;273: 41-51.

[24] Chon MJ, Sethuraman VA, McCormick A, Srinivasan V, Guduru PR. Real-time measurement of stress and damage evolution during initial lithiation of crystalline silicon. *Physical Review Letters.* 2011;107(4): 045503.

[25] Fan F, Huang S, Yang H, Raju M, Datta D, Shenoy VB, Van Duin AC, Zhang S, Zhu T. Mechanical properties of amorphous Li*x*Si alloys: A reactive force field study. *Modelling and Simulation in Materials Science and Engineering.* 2013;21(7): 074002.

[26] Morozov A, Freidin AB, Klinkov VA, Semencha AV, Müller WH, Hauck T. Experimental and theoretical studies of Cu-Sn intermetallic phase growth during high-temperature storage of eutectic SnAg interconnects. *Journal of Electronic Materials.* 2020; 49: 7194-7210.

[27] Freidin AB, Vilchevskaya EN. Chemical affinity tensor in coupled problems of mechanochemistry. In: *Encyclopedia of Continuum Mechanics*. Berlin: Springer; 2019. p.1-17.

[28] Freidin A, Vilchevskaya E, Korolev I. Stress-assist chemical reactions front propagation in deformable solids. *International Journal of Engineering Science.* 2014;83: 57-75.

[29] Morozov A, Khakalo S, Balobanov V, Freidin A, Müller W, Niiranen J. Modeling chemical reaction front propagation by using an isogeometric analysis. *Technische Mechanik.* 2018;38: 73-90.

[30] Poluektov M, Freidin AB, Figiel Ł. Modelling stress-affected chemical reactions in non-linear viscoelastic solids with application to lithiation reaction in spherical Si particles, *International Journal of Engineering Science.* 2018;128: 44-62.

[31] Morozov A, Freidin A, Müller WH, Semencha A, Tribunskiy M. Modeling temperature dependent chemical reaction of intermetallic compound growth. In: *20th International Conference on Thermal, Mechanical and Multi-Physics Simulation and Experiments in Microelectronics and Microsystems* (*EuroSimE*). 2019. p.1-8.

[32] Glansdorff P, Prigogine I, Hill RN. Thermodynamic theory of structure, stability and fluctuations. *American Journal of Physics.* 1973;41: 147-148.

[33] Knyazeva AG. Cross effects in solid media with diffusion. *Journal of Applied Mechanics and Technical Physics*. 2003;44(3): 373-384.

[34] Cui Z, Gao F, Qu J. Interface-reaction controlled diffusion in binary solids with applications to lithiation of silicon in lithium-ion batteries. *Journal of the Mechanics and Physics of Solids*. 2013;61(2): 293-310.

[35] Levitas VI, Attariani H. Anisotropic compositional expansion in elastoplastic materials and corresponding chemical potential: Large-strain for simulation and application to amorphous lithiated silicon. *Journal of the Mechanics and Physics of Solids.* 2014;69: 84-111.

[36] Bower AF, Guduru PR. A simple finite element model of diffusion, finite deformation, plasticity and fracture in lithium ion insertion electrode materials. *Modelling and Simulation in Materials Science and Engineering.* 2012;20(4): 045004.

[37] Timoshenko SP, Gere JS. *Theory of Elastic Stability*. 2nd ed. Mineola: Grover ed.; 1989.

[38] Morozov A, Semencha A, Freidin A, Müller W, Dronova M. Si Nanopowder Based Anode Material for the Lithium Ion Battery Cell. *Key Engineering Materials*. 2019;822: 230-238.